ISSN 2229-5518

Numerical Investigation of Flow Over a Spherical Body at High Reynold's Number

Md. Mamunur Rashid[1], M.G.M. Al Faruque[2]

[1]Department of Mathematics,Hajee Mohammad Danesh Science and Technology University, Dinajpur-5200, Bangladesh
[2]Department of Applied Mathematics, University of Dhaka, Dhaka-1000, Bangladesh

Corresponding author: mamunmath03@gmail.com

Abstract— The paper gives a detail description of flow around a spherical body and its effect many engineering applications under high Reynolds number based on diameter of the sphere. Flow over a sphere at Reynold's number Re≈30000 is investigated in this work with a proper numerical technique. The flow is turbulent and the standard k-ε and the standard k-ω turbulence models are used to capture the turbulent flow behavior of the sphere. Some basic fluid properties of the flow phenomena are discussed with proper contours and diagram and discussed in detail. The downstream complex flow phenomena of the object are observed for both the turbulence models. Using these turbulent models, the paper showed the better agreement to predict the behavior of the flows for the present numerical technique.

Keywords: Sphere, Reynolds number, turbulence, mesh, pressure contour, numerical simulation.

1 Introduction

IN real life problem; flow over a sphere is very important in various engineering applications and energy systems, pollution diffusion, ship hydrodynamics, *etc.* because of its shape [1-2],. Most practical flows such as flow in a river, over a large vehicle, or in the lower atmosphere is almost always turbulent, and the turbulent velocity field is often described as consisting of a large number of eddying motion [3-4]. It is often necessary to develop turbulence models and scaling rules to help predict the behavior of turbulent flows. There are several test cases for computational fluid dynamics, the flow over a spherical body is one of the most challenging and complex flow fields, even though the geometry is simple [5-6]. Therefore, it is beneficial to understand these complex flow phenomena by simulating these simple geometries and predict the behavior of the flows.

The effect of the Reynolds number on the boundary layer on the spherical body can be classified into three categories. When the Reynolds number is below 2×10^5, it is called subcritical range where boundary layer starts as laminar, the separated shear layers are in the early stages of transition, and the wake is fully turbulent [4]. When the Reynolds number reaches above 3.5×10^6 it is called the supercritical region, where the boundary layer starts as laminar, then transitions to turbulent before the separation takes place. The Reynolds number range from 2×10^5 to 3.5×10^6 is called the critical range [7]. As the general shape of a sphere seems to be laminar, our present interest is to investigate the flow over a sphere in turbulent boundary layer at $\mathrm{Re} \approx 3 \times 10^4$.

Many turbulence models were used and developed to investigate the flow characteristics of this type of shape. Observations of flow past a sphere at $\mathrm{Re} = 10^4 \sim 10^8$ by means of oil flow method, the smoke method and the tuft-grid method were examined by Taneda [8] in a wind tunnel test. Wake performance and vortices were observed by him. Achenbach [9] observed vortex shedding from spheres in different critical Re. Vortex shedding from spheres in a uniform flow was observed by Sakamoto and Haniu, [10] at $\mathrm{Re} = 3 \times 10^2 \sim 4 \times 10^4$. Standard hot wire technique was used by them (Sakamoto and Haniu, 1990). These all are experimental set up. To capture the flow around a sphere various turbulence models were used. Large eddy simulation (LES) using unstructured grids was computed by Jindal et al. [11]. Ozgoren et al. [5] investigated the flow characteristics around a sphere over a flat plate in turbulent boundary layer using dye visualization and PIV technique. Direct numerical simulation at low Re around a sphere on subsonic to supersonic flow was investigated also by Nagata et al. 2016. Flow around a sphere placed at various heights was computed using smoke wire and oil flow pattern by Tsutsui [6]. For the interest of flow behavior downstream region of a sphere an experimental set up was done by Ozgoren et al. [12].

To capture the flow characteristics around a sphere at turbulent boundary layer various numerical techniques were used by various scientists. A second-order accurate, finite volume method was used in order to predict the instantaneous and time-averaged flow characteristics using large eddy simulation (LES) on the multi-block grid system which was very well performed result to capture the turbulent flow [9, 13]. In this work a FVM (finite volume method) technique with standard $k-\varepsilon$ and standard $k-\omega$ turbulence models have been used to solve the equations of motion. These results can be used to capitalize on the trend in the design of all engineering applications of fluid mechanic.

2. Methodology

Numerical simulations of the flow around a sphere have been carried out using ANSYS CFD 15 software, in a procedure beginning with creating a geometrical model of the measuring section, generating a discretization mesh and defining all necessary pre-processing parameters, such as boundary condition, turbulent models, fluid properties and other physical parameters. The software used for numerical simulation is based on $k-\varepsilon$ and $k-\omega$ models. The present model is a sphere with diameter H located from upper of the surface. The geometry of the model is given in figure 1. The flow is simulated on the domain surrounded by the sphere is taken as 6 H upstream of the body and 8 H downstream of the body. The lateral side is taken as 6 H and the upper and lower surface is taken as 2 H from the sphere.

ISSN 2229-5518

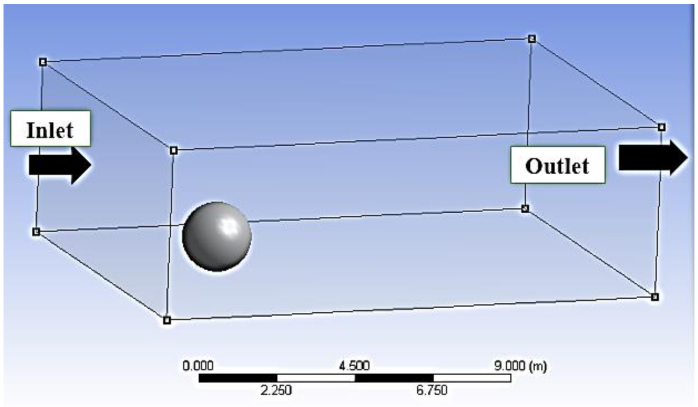

Figure 1: Geometry of the model.

2.1 MESHING

Grid generation is the first step for computational fluid dynamics calculations. The generated discretization mesh is nonuniform, created of approximately 26657 nodes and number of elements of the mesh is 134626, taking into account the structure of the mesh which shown in the figure 2(a). The model was constructed with a grid 0.5 mm in length. The transition ratio is taken as 0.75. The corner view of the 3D mesh of the geometry is showed in Figure 2(b). The sphere was set to solid surfaces with no slip. The working fluid is air.

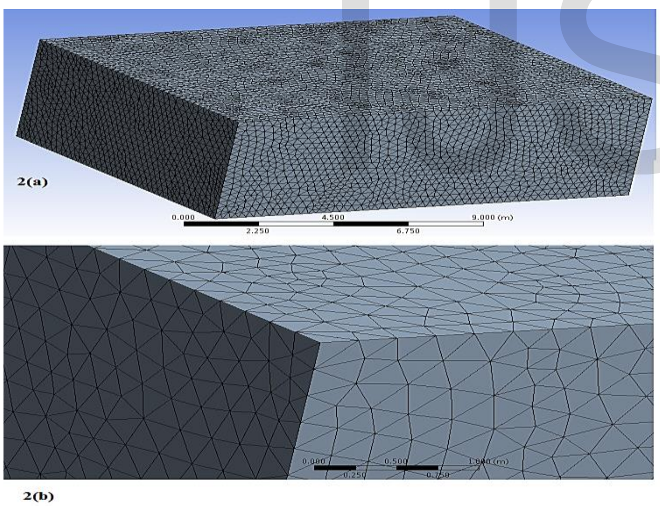

Figure: 2(a) Grid structure in the flow domain 2(b) Meshing at the corner of the geometry

2.2 GOVERNING EQUATIONS

The flow was taken as viscous, turbulent, incompressible and isothermal and the fluid domain is Newtonian (air) having constant property. The turbulence model is using realizable $k-\varepsilon$ and $k-\omega$ because it provides superior performance for flows involving separation and the flow was assumed to be fully turbulent [3]. The flow was also steady and three-dimensional. The equation of continuity and momentum equation, transport equation for $k-\varepsilon$ model, transport equation for $k-\omega$ model are as follows:

The Continuity Equation:

$$\frac{\partial}{\partial x_j}(u_j) = 0\ ;\ j = 1,2,3$$

The Momentum equation:

$$\rho U_j \frac{\partial}{\partial x_j}(U_i) = -\frac{\partial P}{\partial x_j} + \frac{\partial}{\partial x_j}\left[(\mu + \mu_T)\frac{\partial U_i}{\partial x_j}\right];\ i = 1,2,3 \text{ and } j = 1,2,3$$

Here ρ is the fluid density, and μ is the dynamic viscosity, p be the pressure, and μ_T is the turbulent viscosity, respectively.
The turbulent viscosity is given by

$$\mu_T = C_\mu \rho \frac{k^2}{\varepsilon}$$

Where k is the turbulent kinetic energy and ε is the dissipation rate.

The transport equation for $\mathbf{k-\varepsilon}$ model:

The k equation $\rho\frac{\partial}{\partial x_j}(U_j k) = \frac{\partial}{\partial x_j}\left[\left(\mu + \frac{\mu_T}{\sigma_k}\right)\frac{\partial k}{\partial x_j}\right] + P_k - \rho_\varepsilon$

The ε equation $\rho\frac{\partial}{\partial x_j}(U_j \varepsilon) = \frac{\partial}{\partial x_j}\left[\left(\mu + \frac{\mu_T}{\sigma_k}\right)\frac{\partial \varepsilon}{\partial x_j}\right] + \frac{\varepsilon}{k}(C_{\varepsilon 1}P_k - C_{\varepsilon 2}\,\rho_\varepsilon)$

where, $P_k = \mu_T\left(\frac{\partial U_i}{\partial x_j} + \frac{\partial U_j}{\partial x_i}\right)\frac{\partial U_i}{\partial x_j}$; i = 1,2,3 & j = 1,2,3

The Transport equation for $\mathbf{k-\omega}$ model:

k equation: $\frac{\partial}{\partial x_j}(\rho U_j k) = \frac{\partial}{\partial x_j}\left[\left(\mu + \frac{\mu_T}{\sigma_k}\right)\frac{\partial k}{\partial x_j}\right] + P_k - \beta\rho' k\omega$

ω equation: $\frac{\partial}{\partial x_j}(\rho U_j \omega) = \frac{\partial}{\partial x_j}\left[\left(\mu + \frac{\mu_T}{\sigma_\omega}\right)\frac{\partial \omega}{\partial x_j}\right] + \alpha\frac{\omega}{k}P_k - \beta\rho'\omega^2$

2.3 BOUNDARY CONDITIONS

The fluid domain is air at 25^0 c and the fluid was continuous. The reference pressure is taken as 1 atm and the case was non-buoyant whereas the domain was stationary. The flow regime was subsonic, and the inlet uniform velocity was 0.509 m/s. In the pressure outlet, the flow regime was subsonic, and the static pressure was taken as 0 pa.

Constants used in the entire turbulence models:

For $k-\varepsilon$:
C_μ =0.09, $C_{\varepsilon 1}$=1.44, $C_{\varepsilon 2}$=1.92, σ_k=1.0, σ_ε=1.3
For $k-\omega$:
α=5/9, σ_k=2.0, σ_ω=2, β=0.075,β′=0.09

2.4 NUMERICAL SOLUTION

Reynolds averaged Navier-Stokes equations have been widely used in prediction of turbulent flows. A second order upwind pressure velocity coupling SIMPLE algorithm is used to solve the governing Navier Stokes equations. A commercial CFD software Ansys Fluent 15.0 is utilized to solve these equations. The simulation was run until the residual of the pressure and velocities were less than 10^{-4} for both simulations.

3 RESULTS AND DISCUSSION

A spherical body in a crossflow at Reynolds number $Re=3\times10^4$ is simulated. The results were observed in fully turbulent flow. Various fluid properties were observed for various conditions whereas some important view and observations were mentioned here. Figure 2(a) shows the velocity vector for $k-\epsilon$ model. It shows the direction of velocity. It is clear from figure that the speed of velocity is lower at upstream and downstream of the sphere. It is very high at the upper and lower surface of the sphere. Figure 2(b) shows the velocity streamline for $k-\omega$ model. It shows that there exists a wake region downstream of the sphere. Figure 3 shows the pressure contour over the cylinder for both the $k-\varepsilon$ and $k-\omega$ models. For both the model the pressure was very high in front of the sphere and very low at the upper and lower surface of the sphere. The pressure was average at the whole domain. At the front contact surface, the pressure was highest. Velocity contour for both the model was showed in figure 4. Since the air was acting in front of the sphere; velocity was very low their and same as the downstream region. The velocity was very high at the upper and lower surface of the sphere since the airflow was passing by that region. Velocity profile at the front, mid and upper surface of the sphere was showed in figure 5,6 and 7. The velocity profile was found nearest same for both the $k-\varepsilon$ and $k-\omega$ model. This velocity profile suggested that the velocity was high enough at the upper mid surface and gradually lower on the front and back surface.

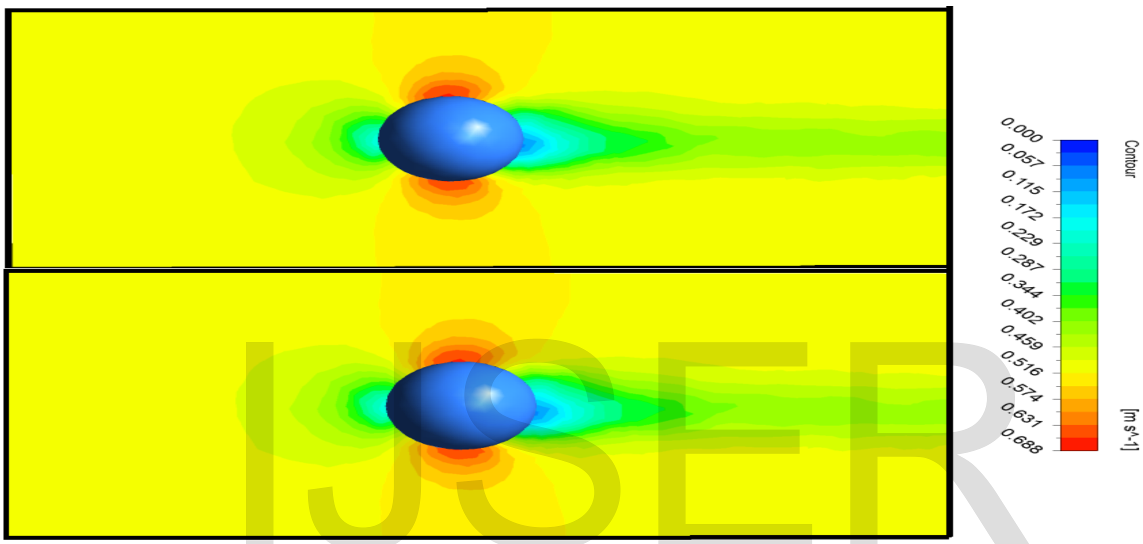

Figure 3: Velocity contour for $k-\varepsilon$ and $k-\omega$ model around the spheres.

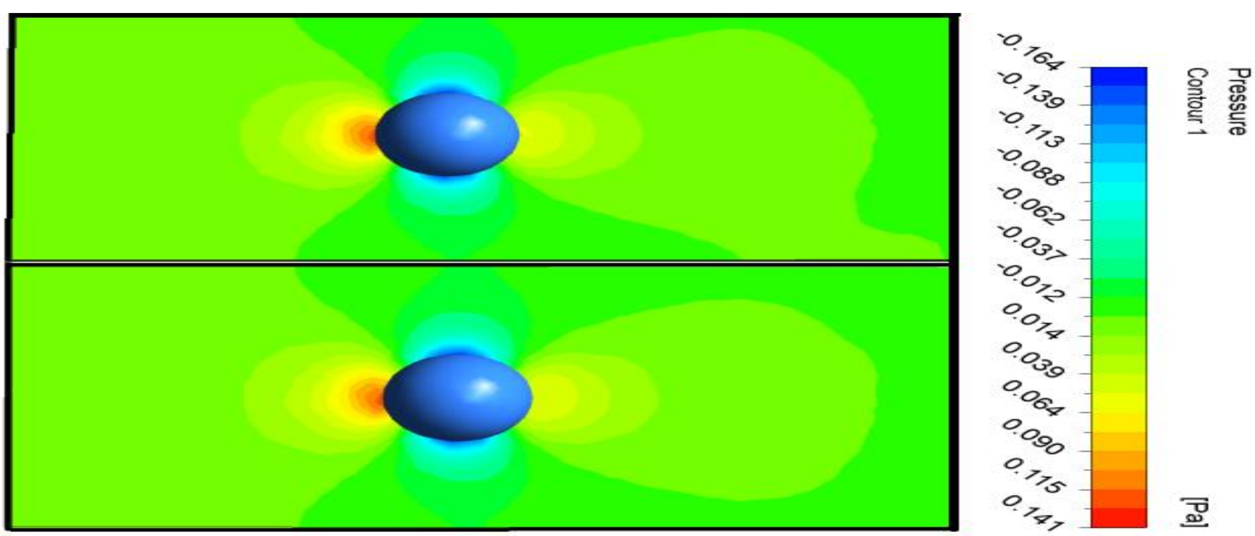

Figure 4: Pressure contour for $k-\epsilon$ and $k-\omega$ model around the spheres.

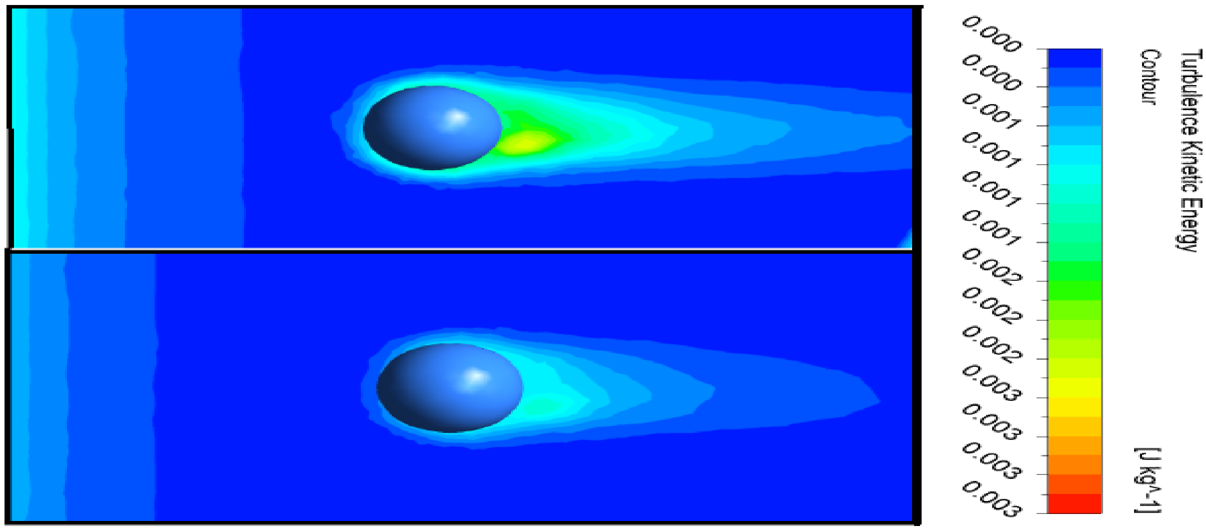

Figure 5: Turbulent kinetic energy for the $k-\varepsilon$ and $k-\omega$ model.

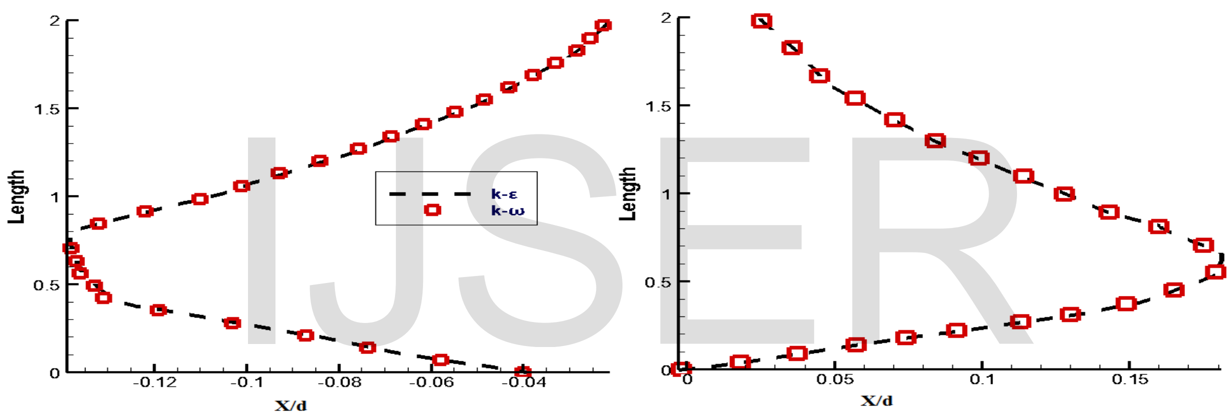

Figure 6: Velocity vs. Length profile at the back(left) and front (right) surface (W/H=1) of the sphere

The concept of flow separation and recirculation was observed from figure 5 and 6. Since the pressure was very low in the lower surface of the sphere; fluid (air) was taken place on that surface and resulted a recirculation region in that place. The recirculation zone was also observed in the nearest upstream and downstream of the sphere. Since the flow was acting in front of the sphere; flow separation occurred there. Flow separation and recirculation region was also observed from figure 6. Flow separation of the present flow phenomena occurred upstream of the sphere due to the adverse pressure gradient or the velocity of the fluid subject to the sphere tends to zero.

Table-1 reads the area average property on the symmetry plane of the sphere for both the turbulence model.

Table 1 Area average property on the symmetric plane of the sphere.

Turbulence model	Velocity $[ms^{-1}]$	Pressure [pa]	Turbulent kinetic energy $[jkg^{-1}]$	Eddy viscosity [Pas]
$k-\varepsilon$	0.488774	0.00254132	0.000309063	0.000232994
$k-\omega$	0.488948	0.0026299	0.000249353	0.000175523

4 Conclusion

Two turbulence model $k-\varepsilon$ and $k-\omega$ are used to predict the flow and calculate the numerical simulation over a sphere for the Reynolds number 3 ×

10^4. A structured mesh topology was constructed to mesh the sphere along the surrounding domain. Results using both the model showed that the pressure acting in the front surface of the sphere was higher than the downstream. And velocity was very high at the upper and lower surface of the cylinder. Some complex flow phenomena like flow separation which occurred in front of the sphere and recirculation region which occurred on the upper and lower surface of the sphere was also observed. This observation clarifies the high Reynold's number flow or the turbulent behavior of the flow. The second order upwind based SIMPLE algorithm had a good contribution solving the equations of motions. This turbulent flow phenomenon over the sphere depicted that a complex flow or a wake region occurs downstream of the sphere or this type of bluff structures.

REFERENCES

[1] Kotsev, T., 2018. Viscous flow around spherical particles in different arrangements, MATEC web of conferences 145, doi.org/10.1051/matecconf/201814503008.

[2] Lo, S.C., K.A.Hoffmann, and J.F.Dietiker, 2005. Numerical investigation of high Reynolds number flows over square and circular cylinders, Journal of Thermophysics and heat transfer, vol 19(1), DOI: 10.2514/1.9195.

[3] Yen,C.H., U.J. Hui, Y.Y.We, A. Sadikin, N.Nordin, I. Taib, K.Abdullah, A.N.Mohammed, A Sapit, M.A.Razali, 2017. Numerical study of flow past a solid sphere at high Reynolds number, IOP conference series: Material science and engineering 243, doi:10.1088/1757-899X/243/1/012042.

[4] Hultmark, M., M. Valikivi, S.C.C. Bailey, and A.J.Smits, 2012. Turbulent pipe flow at extreme Reynolds numbers, Physical review letters, 108, DOI: 10.1103/PhysRevLett.108.094501.

[5] Ozgoren M, Okbaz A, Dogan S, Sahin B and Akilli H. 2013. Investigation of flow characteristics around a sphere placed in a boundary layer over a flat plate; Experimental Thermal and Fluid Science 44,62–74.

[6] Tsutsui T. 2008. Flow around a sphere in a plane turbulent boundary layer, Journal of Wind Engineering and Industrial Aerodynamics 96, 779–792.

[7] Nagata T, Nonomura T, Takahashi S, Mizuno Y and Fukuda K. 2016. Investigation on subsonic to supersonic flow around a sphere at low Reynolds number of between 50 and 300 by direct numerical simulation Physics of fluids 28, 056101

[8] Taneda S. 1978. Visual observations of the flow past a sphere at Reynolds numbers between 10^4 and 10^5 J. Fluid Mech. vol. 85, part 1, pp. 187-192.

[9] Achenbach E. 1974. Vortex shedding from spheres, J. Fluid Mech. vol. 62, part 2, pp. 209-221.

[10] Sakamoto H and Haniu H. 1990. A Study on Wortex Shedding from Spheres in a Uniform Flow ASME Vol. 112 pp. 386-392

[11] Jindal S, Long LN, Plassmann PE and Sezer-Uzol N. 2004. Large eddy simulation around a sphere using unstructured grids. AIAA. 22-28.

[12] Ozgoren M, Pinar E, Sahin B and Akilli H. 2011. Comparison of flow structures in the downstream region of a cylinder and sphere; International Journal of Heat and Fluid Flow 32 ,1138–1146.

[13] Hassanzadeh R, Sahin B and Ozgoren M. 2011. Numerical investigation of flow structures around a sphere, International Journal of Computational Fluid Dynamics, 25:10, 535-545.